Effects of Mo substitution for Ni on the microstructure and property of V-based hydrogen storage alloys

Yanwei Tong[1,a] and Lin Deng[1]

[1]*College of Biology and Chemistry Engineering, Panzhihua University, Panzhihua 617000, China*

Abstract. In order to study the property the V-based hydrogen storage alloys, Ni in the alloys was partially substituted by Mo. The $V_2Ti_{0.5}Cr_{0.5}Ni_{1-x}Mo_x$ (x=0.02-0.08) hydrogen storage alloys were prepared by induction melting, and the effects of Mo content on the microstructure and electrochemical property were investigated systematically. The results show that the alloys mainly consist of a V-based solid solution phase with a BCC structure and a TiNi-based secondary phase. The electrochemical measurements indicate that with increasing the content of Mo, the maximum discharge capacity, the cycle stability and high rate discharge ability is increased first and then decreased.

1 Introduction

Hydrogen storage alloys used as negative electrode materials in Ni/MH secondary batteries are extensively studied in the past decades and a series of metal hydride electrode materials have been discovered, such as rare-earth-based AB_5-type alloys [1], AB_3-type rare-earth-based alloys [2], AB_2-type Laves phase alloys [3], Mg-based alloys [4], and V-based solid solution alloys [5,6]. As one kind of metal-based hydrogen storage alloys, V-based solid solution alloys have exhibited highly attractive properties for practical application because of their higher hydrogen storage capacity and lower hydrogen absorption/desorption temperature [7-9]. However, the V-based hydrogen storage alloy exhibited poor charge-discharge cycle stability because of the dissolution of the V constituent in the electrolyte. In order to improve the cycle stability of this type of alloy, the investigations of the element substitution and additive [10-12] were conducted. Some researchers have studied the influence of Mo additive in AB_5-type alloys [13,14], but the research of influence of Mo additive in V -based hydrogen storage alloys is seldom.

In this study, we prepared $V_2Ti_{0.5}Cr_{0.5}Ni_{1-x}Mo_x$ (x=0.02-0.08) alloys in which Mo was partially substitution for Ni, in order to improve the charge-discharge cycle stability of $V_2Ti_{0.5}Cr_{0.5}Ni$ alloy. Characteristics of the battery performance, such as discharge capacity, cycle stability and high-rate dischargeability were evaluated.

.

2 Experimental

The purity of raw materials is as follows: V>99.9wt.%, Ti>99.9wt.%, Cr>99.9wt.%, Ni>99.9wt.%, Mo>99.9wt.%, respectively. The alloys were arc-melted in the water-cooled copper crucible under argon atmosphere (purity, 99.999 wt.%). To ensure the homogeneity, the alloys were turned over and remelted for five times. The samples were mechanically crushed into fine powders of 200-320 mesh in mortar for X-ray diffraction (XRD) and electrochemical measurements analysis. The XRD data was collected by a step-scanning method using DX-2700 with CuKα .

The well-mixed alloy powder and carbonyl nickel powder in weight ratio of 1:4 was compacted onto an expanded nickel substrate by a 10 MPa to form a test electrode (about diameter of 10 mm, thickness of 1 mm) without binder.

The electrochemical property was performed on LAND battery testing instrument using a tri-electrode system consisting of a working electrode (MH electrode), a sintered $Ni(OH)_2$/NiOOH counter electrode with excessive capacity and a reference electrode (Hg/HgO, OH-). The electrolyte in the cell was 7 mol/L KOH aqueous solution. The electrode was charged for 6 h at a constant current density (100 mA/g) followed by 5 min resting time and then discharge at a constant current density (60 mA/g) to a cutoff potential of -0.6 V at 303 K.

3 Results and discussion

3.1. Alloy structure characteristic

[a] Corresponding author: 317435736@qq.com

The typical X-ray diffraction patterns of the $V_2Ti_{0.5}Cr_{0.5}Ni_{1-x}Mo_x$ (x=0.02-0.08) alloys are shown in Figure1. It can be seen that all of the alloys exhibit similar diffraction patterns, indicating that the phase constitutions of the alloys are a V-based solid solution phase with a BCC structure and a TiNi-based secondary phase. With increasing the content of Mo, the diffraction peak intensity of V-based solid solution phase increases.

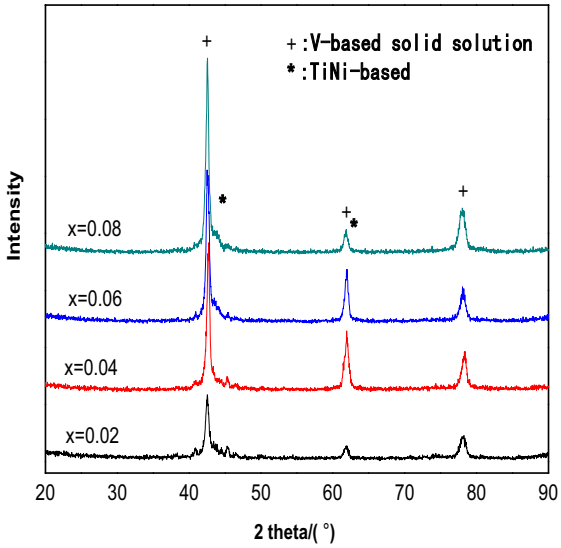

Figure 1. XRD pattern of the $V_2Ti_{0.5}Cr_{0.5}Ni_{1-x}Mo_x$ (x=0.02-0.08) alloys

The metallographs of $V_2Ti_{0.5}Cr_{0.5}Ni_{1-x}Mo_x$ (x=0.02-0.08) alloy electrodes are shown in Figure 2. It displays that all of the alloy samples are mainly composed of two distinct crystallographic phases: the 3-D interpenetrating phase is the TiNi-based phase, and the dendritic phase is the V-based solid solution phase. Akiba et al [15] pointed out that 3-D interpenetrating TiNi-phase could collect electrons and worked as a catalyst for the BCC phase which has a high absorption hydrogen capacity. The TiNi-based phase with 3-D network structure was very important for the electrochemical kinetics of the alloy electrodes.

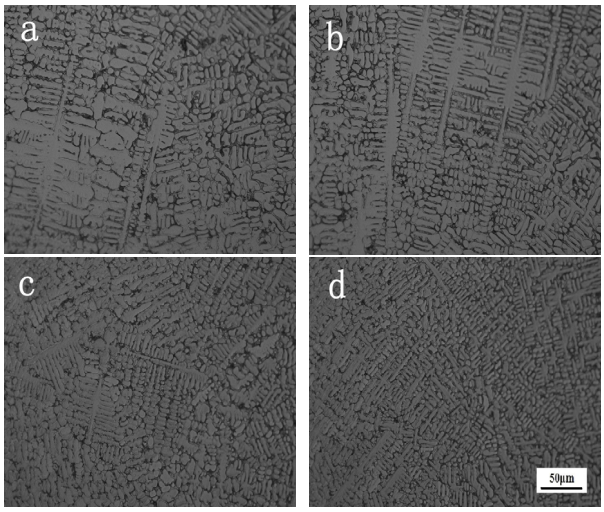

Figure 2. Metallographs of the $V_2Ti_{0.5}Cr_{0.5}Ni_{1-x}Mo_x$ (x=0.02-0.08) alloys. (a)x=0.02; (b)x=0.04; (c)x=0.06; (d) x=0.08

3.2 Discharge capacity and cycle stability

The curves of the discharge capacity versus the cycle number at 303 K for $V_2Ti_{0.5}Cr_{0.5}Ni_{1-x}Mo_x$ (x=0.02-0.08) alloy electrodes are shown in Figure 3. It can be seen that after the substitution of Mo for Ni, the activation property of the alloy electrodes is decreased. The maximum discharge capacity (C_{max}) and the rate of capacity retention S_{20} (S_{20} is defined as $S_{20}= C_{20}/C_{max} \times 100\%$, where C_{20} is the discharge capacity measured at the 20th cycle) of the alloy electrodes are summarized in Table 1. It can be seen that with increasing the content of Mo substitution for Ni, the maximum discharge capacity of the alloy electrodes increased from 362.5 mAh/g (x=0.02) to 385.7 mAh/g (x=0.06) and then decreased to 340.3 mAh/g. The rate of capacity retention S20 first increased from 80.4% to 85% and then decreased to 79.4%, which means that a proper component ratio of Mo substitution for Ni is benefit to the maximum discharge capacity and the cycle stability of the alloys. Maybe a proper component ratio of Mo substitution for Ni resists the dissolution of alloy element and increases the anti-corrosion of the alloy.

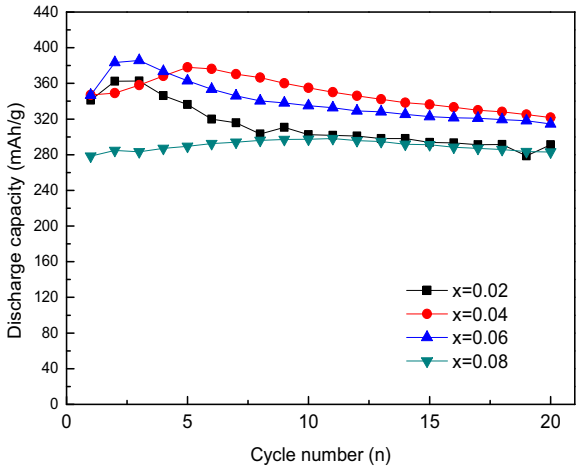

Figure 3. Discharge cycling performance of the $V_2Ti_{0.5}Cr_{0.5}Ni_{1-x}Mo_x$ (x=0.02-0.08) alloy electrodes

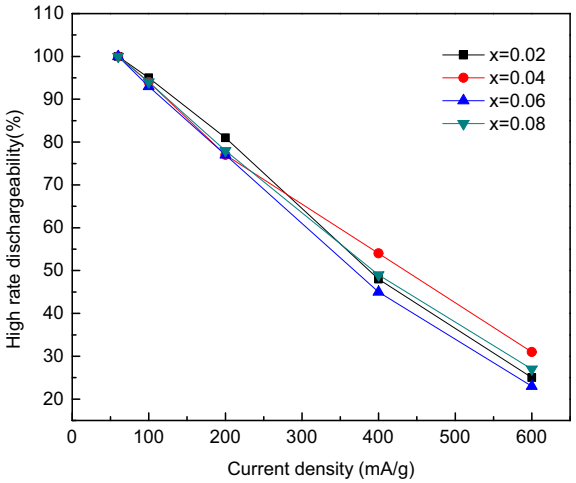

Figure 4. High rate discharge ability of the $V_2Ti_{0.5}Cr_{0.5}Ni_{1-x}Mo_x$ (x=0.02-0.08) alloy electrodes

3.3 High rate discharge ability

The high rate discharge ability (HRD) is measured at different discharge current densities (60 mA/g, 100 mA/g, 200 mA/g, 400 mA/g, 800 mA/g). The HRD is dendined as

$$HRD = \frac{C_n}{C_{\max}} \quad (1)$$

where C_{max} represents the maximum discharge capacity at a discharge current density of 60 mA/g, and C_n is the discharge capacity at a discharge current densities (n=60, 100, 200, 400, 800).

Figure 4. shows the high rate discharge ability (HRD) of the $V_2Ti_{0.5}Cr_{0.5}Ni_{1-x}Mo_x$ (x=0.02-0.08) alloy electrodes. The HRD is measured at different discharge current densities (60mA/g, 100mA/g, 200mA/g, 400mA/g, 600mA/g). It can be found that the HRD of the alloy electrodes decreases with increasing discharge current density, while with increasing the content of Mo substitution for Ni, the HRD first increases and then decreases. It is generally accepted that the high-rate dischargeability of a metal hydride electrode is mainly determined by the charge transfer process occurring at the metal electrolyte interface and/or the hydrogen diffusion process in the hydride bulk [16]. The substitution of Mo for Ni may improve the charge transfer and the hydrogen diffusion process.

Table 1. Electrochemical behavior of the $V_2Ti_{0.5}Cr_{0.5}Ni_{1-x}Mo_x$ (x=0.02~0.08) alloy electrodes

Samples	C_{max} (mAh/g)	S_{20} (%)	HRD (C_{400}/C_{60}) (%)	I_0 (mA/g)
x = 0.02	362.5	80.4	48	54
x = 0.04	378.0	85.0	54	68
x = 0.06	385.7	81.5	45	60
x = 0.08	340.3	79.4	49	38

The exchange current density (I_0) of $V_2Ti_{0.5}Cr_{0.5}Ni_{1-x}Mo_x$ (x=0.02-0.08) alloy electrodes is a measure of the forward and reverse electrode reaction rate at the equilibrium potential. It can be used to characterize electrocatalytic activity of the electrode surface. A high exchange current density means a high electrochemical reaction rate with good cyclic performance. The exchange current density may be calculated from the polarization resistance (R_p) using the simplified Butler-Volmer equation at low overpotential limit conditions as follows:

$$I_0 = \frac{RT}{FR_p} \quad (2)$$

Where R is the gas constant (J/(mol K)), T is the absolute temperature (K) and F is the Faraday constant (C/mol). The polarization resistance $1/R_p$ can be obtained from the linear polarization curves of the oxide electrode

as shown in Figure 5. And the calculated current density is listed in Table 1, respectively.

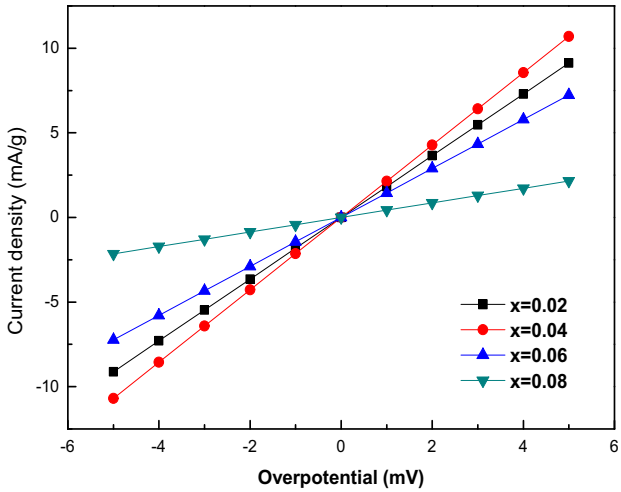

Figure 5. Linear polarization curves of $V_2Ti_{0.5}Cr_{0.5}Ni_{1-x}Mo_x$ (0.02-0.08) alloy electrodes

4 Conclusions

The structural and electrochemical properties of the $V_2Ti_{0.5}Cr_{0.5}Ni_{1-x}Mo_x$ (x=0.02-0.08) alloy electrodes have been systematically studied. All of the alloys are composed of a V-based solid solution phase with a BCC structure and a TiNi-based phase. With increasing the content of Mo substitution for Ni, the maximum discharge capacity (C_{max}) , the rate of capacity retention (*HRD*), the high-rate dischargeability and the exchange current density (I_0) of the alloy electrodes increase first and then decrease, and reach the best performance with x=0.04.

References

1. Liu YF, Zhang SS, Li R, Gao MX, Zhong K, Miao H, et al. Int J Hydrogen Energy **33**, 728 (2008)
2. Kohno T, Yoshida H, Kawashima F, Sakai I, Yamamoto M, Kanda M. J. Alloys Compd. **311**, 5 (2000)
3. Ovshinsky SR, Fetcenko MA, Ross J. Science **260**, 176 (1993)
4. Wang FX, Gao XP, Lu ZW, Ye SH, Qu JQ, Wu F, et al. J Alloys Compd. **370**, 326 (2004)
5. Tsukahara M, Kamiya T, Takahashi K, Kawabata A, Sskurai S, Shi J. J Electrochen Soc **147**, 2941 (2000)
6. Tong YW, Gao JC, Deng G, et al. Materials Letters **112**, 142(2013)
7. Tsukahara M, Takahashi K, Mishima T, Sakai T, Miyamura H, Kuriyama N. J Alloys Compd **224**, 162 (1995)
8. Song XP, Pei P, Zhang PL, Chen GL. J Alloys Compd **455**, 392 (2008)
9. Tong YW, Gao JC, Deng G, et al. Rare Metal Materials and Engineering **44**, 1052 (2015)
10. Parimala R, Ananth MV, Ramaprabhu S. Int J Hydrogen Energy **29**, 509 (2004)
11. Liu FJ, Suda S. J Alloys Compd. **231**, 666 (1995)
12. Wang YZ, Zhou MS. Journal of Rare Earths **30**, 146 (2012)
13. Yeh MT, Beibutian VM, Hsu SE. J Alloys Compd. **293**, 721 (1999)
14. Yang SQ, Han SM, Song JZ, Li Y. J Rare Earths **29**, 692 (2011)
15. Akiba E, Iba H. Intermetallics **6**, 467 (1998)
16. Li SC, Zhao MS, Wang LM, Liu Y, Wang YZ. Mater. Sci. Eng., B ; **150**, 168 (2008)